Journal of Ecology of Health & Environment
An International Journal

http://dx.doi.org/10.12785/jehe/010104

A finite Element Model for the Electrical Activity in Human Cardiac Tissues

Shuaiby M. Shuaiby[*], *M. A. Hassan, Abdel-Badie Sharkawy and Abdel-Rasoul M.M.Gad*

Mechanical Engineering Department, Faculty of Engineering, Assiut University, Assiut, Egypt.

Received: 24 Jun. 2012, Revised: 7 Nov. 2012, Accepted: 14 Nov. 2012
Published online: 1 May. 2013

Abstract: Biosimulation models of the heart action potential have become a very useful tool. It provides better understanding for the complex biophysical phenomena related to electrical activity in the heart such as cardiac arrhythmias. At cellular level, the electrical activity of cardiac tissues may be simulated by solving a system of ordinary deferential equations (ODEs) describing the electrical behavior of the cell membrane. Because the biophysical processes underlying this phenomenon are non-linear and change very rapidly, the ODE system is a challenge to be solved numerically. Furthermore, the implementation of these models is a hard task for commercial finite element software. In this paper a finite element formulation, model and code generation of monodomain equation has been conducted. The developed code is coupled with the modified FitzHugh-Nagumo (FHN) cell electrophysiological model in order to have isotropic excitation propagation starting from cell level to complete heart level. MTALAB programming language was used to build the proposed standalone finite element code. A two dimensional specimen of heart tissues is simulated to show the behavior of the excitation propagation and the repolarization phase for isotropic electrical activity. Simulation results of the cardiac action potential have shown good agreements with the experimental measurements obtained from published literature.

Keywords: Action potential, Cardiac Electrical modeling, Finite element method.

1 Introduction

Modeling of the electrical activation of the heart allows us to test if our knowledge of small-scale phenomena, such as the behavior of the cardiac membrane, suffices to explain large-scale phenomena, such as the electrocardiogram (ECG). Cardiac diseases are a major cause of death in the world, and a lot of work has been done to elucidate the causes and mechanisms of heart problems [1].Computer models have become valuable tools for the study and comprehension of the complex phenomena of cardiac electrophysiology. The models have played an important role in this field [2] and support the tests of new drugs, the development of new medical devices and non-invasive diagnostic techniques.

Electrical activity is responsible for the periodic contraction and relaxation cycle of the cardiac that propels blood throughout the body. Hence, electrical activity is essential for the cardiac to perform its function. Most serious cardiac problems are in fact related to disturbances in the cardiacs electrical activity [3].

Electrophysiological models of the cardiac describe how electricity flows through the cardiac, controlling its contraction. The models in which we are interested consist of systems of deferential equations. Models of the electrophysiology of one cell are governed by systems of ordinary deferential equations (ODEs), and models of the electrophysiology of tissue are governed by one or more partial deferential equations (PDEs) [3].Typically, a PDE models coupled with an ODE model to simulate cardiac tissue consisting of a network of cells. The ODEs model the electrical activity in the cells, and the PDEs model the propagation of the electrical activity across the network as a whole.

The electrical activity of the cardiac as a whole is thus characterized by a complex multiscale structure, ranging from the microscopic activity of ion channels in the cellular membrane to the macroscopic properties of the anisotropic propagation of the excitation and recovery fronts in the whole cardiac. The most complete model of such a complex setting is the anisotropic bidomain model [4], that consists of a system of two degenerate parabolic reaction diffusion equations describing the intra and extracellular potentials in the cardiac muscle, coupled with a system of ordinary deferential equations describing

[*] Corresponding author e-mail: shuaib_eng@yahoo.com

the ionic currents flowing through the cellular membrane, that are associated to the nonlinear reaction term. This model is computationally very expensive because of the involvement of different space and time scales. A simplified tissue model of the anisotropic monodomain system, consisting of a parabolic reaction diffusion equation describing the propagation of the transmembrane potential coupled with an ionic model, has been widely used in literature [5,6].

The aim of the present work is to model and simulate action potential in human cardiac tissue as powerful tools in the study of cardiac arrhythmias. The technique of finite element method has been used to build a computer program to solving the phenomena of excitation propagation for isotropic electrical activity. The result of the proposed stand alone finite element code model compared with [12,16] show good agreement with the experimental measurements of the action potential of the cardiac tissue. The relative root-mean square error is less than 5%, which is generally considered acceptable.

The rest of the paper is organized as follows. Section 2 describes the ionic membrane models and the modified FHN membrane models. Section 3 formulates the bidomain model. Section 4 formulates the monodomain model. Section 5 describes the conductivity tensors. Section 6 describes the boundary conditions. In Section 7, numerical simulation results of the monodomain model are presented and analyzed. In Section 8 offers our conclusion.

2 Models of cardiac cell memberane

2.1 Ionic memberane models

Ionic membrane models describe the mean behavior of the ionic channels in a small membrane patch containing a number of the latter large enough to observe their statistical evolution through time [4]. The first membrane model for ionic currents appearing in both the monodomain and the bidomain model relies on the choice of the membrane model for the cell conductivity. The membrane model includes three components connected in parallel as depicted in Fig. 1.

The total transmembrane current Im can be expressed as:

$$I_m = C_m \frac{\partial V_m}{\partial t} + I_{ion} - I_{stim} \tag{1}$$

Where V_m is the transmembrane potential defined as the difference between the intracellular and extracellular potentials ϕ_i and ϕ_e, Iion is the sum of all transmembrane ionic currents, I_{stim} is the externally stimulus current, and C_m is the total membrane capacitance. In the case of an isolated cell or isolated membrane patch no currents can flow in the intracellular medium, $I_m = 0$. The formulation is in this case equivalent to the HodkingHuxley

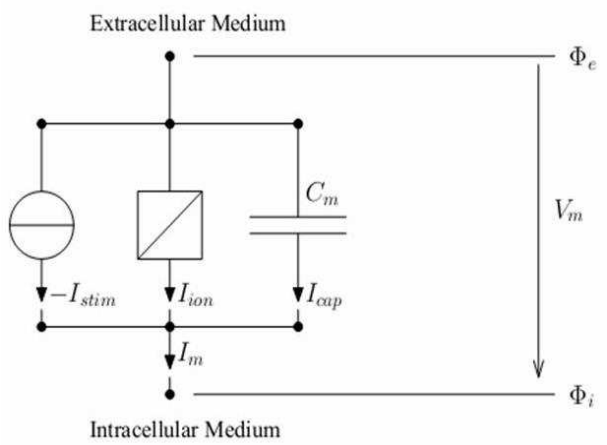

Fig. 1: Equivalent current source model for the cardiac membrane.

formulation for nerve cells [7] and the transmembrane potential evolution can be written:

$$\frac{\partial V_m}{\partial t} = -\left(\frac{I_{ion} - I_{stim}}{C_m}\right) \tag{2}$$

2.2 The modified fitzhugh-nagumo cell model

FitzHugh and Nagumo reduced the HodgkinHuxley equation (four-dimensional) to a two-dimensional system by extracting the excitability of dynamics in the original HodgkinHuxley equation [8]. Here after, the simplest ionic model is the FitzHugh-Nagumo (FHN), consisting of one ionic current and one gating variable. Assuming the potential V to be zero at rest, the ionic current uses only one recovery variable:

$$I_{ion} = cu(u-\alpha)(u-1) + w \tag{3}$$

$$\frac{\partial w}{\partial t} = \varepsilon(u - \gamma w) \tag{4}$$

Here w is a recovery variable and is the normalized transmembrane potential, defined by

$$u = \frac{v_m - v_{rest}}{v_p - v_{rest}} \tag{5}$$

where v_m is the transmembrane potential, v_{rest} is the resting potential, and v_p is the plateau potential [9]. The normalized threshold potential α is defined in a similar way

$$\alpha = \frac{v_{th} - v_{rest}}{v_p - v_{rest}} \tag{6}$$

where, v_{th} is the threshold potential.

3 Mathematical derivation of the bidomain model

The most substantial mathematical description of the bidomain model is found in the review paper [4], which present a definition of the model from its origins in the core conductor model. Heart tissue can be classified into two groups: intracellular and extracellular as shown in Fig 2. To account for the effects of potential differences across the cell membrane, the bidomain model treats these two groups as two separate domains. Each point in the heart is considered to be in both domains, which can be thought of as superimposed on one another [10]. Each point has an electrical potential field in each domain [3].

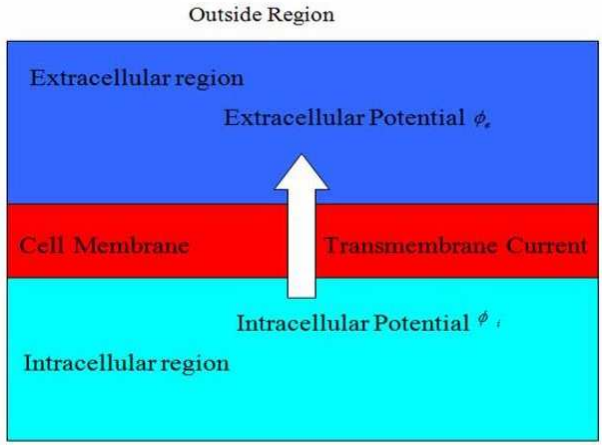

Fig. 2: The bidomain model

The bidomain model of cardiac tissue is based on current flow, distribution of electrical potential, and the conservation of charge and current [4]. The description of each domain is based on a generalized version of Ohms law defining the relationship between the electric field E, derived from the potential $\phi(V)$, the current density J and the conductivity tensor D. A discrete interpretation of the bidomain equations is given for a 1D cable in Fig. 3.

$$E = -\nabla\phi$$
$$J = DE = -D\nabla\phi \tag{7}$$

Considering the intracellular and extracellular spaces specifically, we have:

$$J_i = -D_i\nabla\phi_i$$
$$J_e = -D_e\nabla\phi_e \tag{8}$$

where J_i and J_e are the intracellular and extracellular current densities, D_i and D_e are the corresponding conductivity tensors, respectively, and ϕ_i and ϕ_e are the electrical potential in the intracellular and extracellular spaces.

$$\nabla.J_i = -I_m, \qquad \nabla.J_e = I_m$$
$$\nabla(J_i + J_e) = 0 \tag{9}$$

where I_m is transmembrane current per unit volume [11], which is composed of a capacitive component, and an ionic component I_{ion}.

$$I_m = \beta_m\left(C_m\frac{\partial V_m}{\partial t} + I_{ion} + I_{app}\right) \tag{10}$$

where β_m is the surface area- to-volume ratio of a cardiac cell, C_m the specified cell membrane capacitance,I_{app} is the stimulus current and V_m is the transmembrane voltage which is given by:

$$V_m = \phi_i - \phi_e \tag{11}$$

Combining Equations (9) (11), we obtain:

$$\nabla.D_i\left(\nabla V_m + \nabla\phi_e\right) = \beta_m\left(C_m\frac{\partial V_m}{\partial t} + I_{ion} + I_{app}\right) \tag{12}$$

$$\nabla.((D_i + D_e)\nabla\phi_e) = -\nabla.(D_i\nabla V_m) \tag{13}$$

The parabolic (12) and elliptic (13) equations are the governing equations of the biodomain model of cardiac tissue.

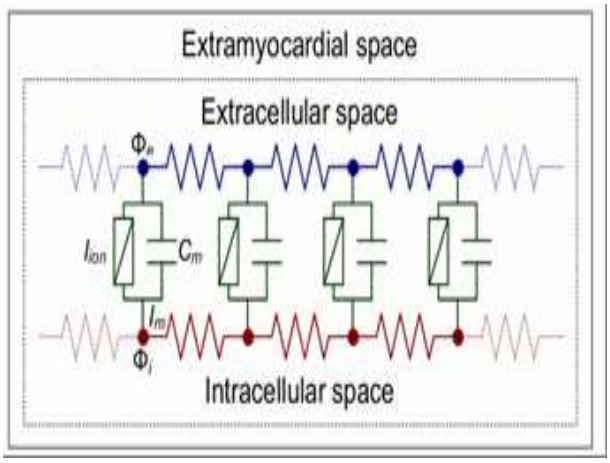

Fig. 3: A discrete equivalence of the bidomain formulation for a 1D continuous cable.

In Fig. 3., the membrane components correspond to Fig. 1, but the I_{stim} current source has been discarded to simplify the presentation.

4 Mathematical derivation of the monodomain model

The monodomain model is a simplification of the bidomain model that is easier to analyze and less computationally demanding [3]. A discrete interpretation of the monodmain equations is given for a 1D cable in Fig. 4. In this analysis, we assume that the anisotropy of the intracellular and extracellular spaces is the same, i.e. that the conductivity in the extracellular space is proportional to the intracellular conductivity.

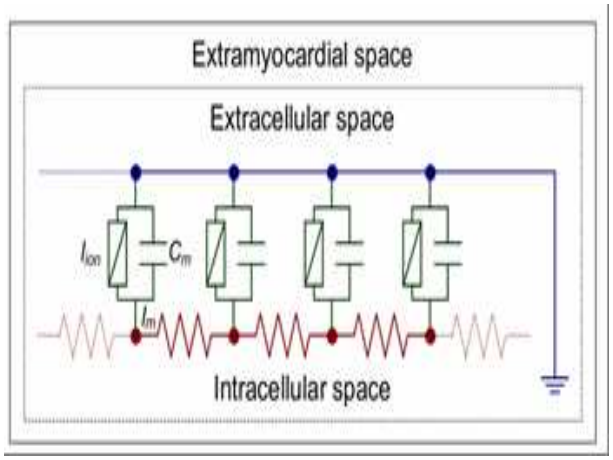

Fig. 4: A discrete equivalence of the monodomain formulation for a 1D continuous cable, similar to the bidomain equivalence of Fig. 3.

$$D_e = \lambda D_i \tag{14}$$

where, $\lambda$is a scalar, representing the ratio between the conductivity of the intracellular and extracellular spaces. The choice of the value of λ can determine physiological accuracy, but it is important to select a suitable value that gives the satisfactory results [3]. The computational cost of using the monodomain model is about one-half to one-tenth the cost of using the bidomain model [12,6], depending on the complexity of the cell model used.

Substituting equation (14) into equation (13) gives:

$$\nabla.((D_i + \lambda D_i)\nabla\phi_e) = -\nabla.(D_i\nabla V_m) \tag{15}$$

$$\nabla.(D_i\nabla\phi_e) = -\frac{1}{1+\lambda}\nabla.(D_i\nabla V_m) \tag{16}$$

Substituting equation (16) into equation (12) gives:

$$\nabla.\frac{1}{1+\lambda}D_i\nabla V_m = \beta_m\left(C_m\frac{\partial V_m}{\partial t} + I_{ion} + I_{app}\right) \tag{17}$$

If we introduce an effective conductivity $D = \frac{\lambda}{1+\lambda}D_i$,[13] we obtain the monodomain model of cardiac tissue as:

$$\nabla.D\nabla V_m = \beta_m\left(C_m\frac{\partial V_m}{\partial t} + I_{ion} + I_{app}\right) \tag{18}$$

$$\frac{\partial V_m}{\partial t} = -\frac{1}{C_m}(I_{ion} + I_{app}) + \left(\frac{1}{C_m\beta_m}\right)\nabla.D\nabla V_m \tag{19}$$

5 Connectivity tensor

The conductivity tensor D in equation (19) is defined largely by the structure of the heart. Cardiac cells are grouped into muscle fibers, and the muscle fibers are grouped into sheets of fibers [4]. See Fig. 5. The structure of the heart influences the flow of electricity. Conductivity is usually greater along the fibers rather than across them, [3].

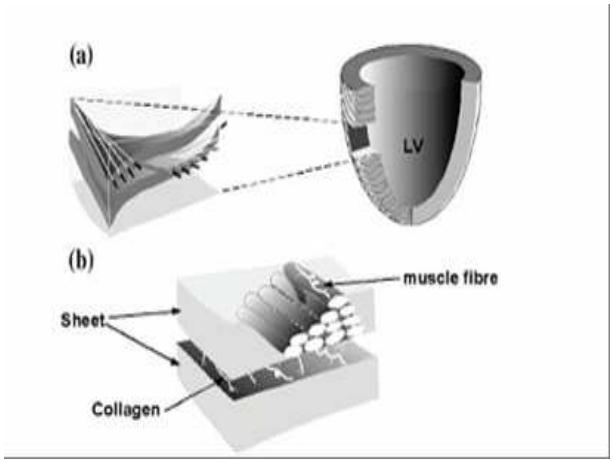

Fig. 5: The cross section of muscle fiber in the left ventricle (LV), illustrating (a) the change in the direction of muscle fiber throughout the heart wall and (b) the grouping of fibers and sheets.

At each point in the extracellular and intracellular domain a local conductivity tensor, denoted D_{nfo}, the conductivity tensor for the case where there is no fiber orientation can be represented by a symmetric matrix and defined in the basis formed as.

$$D_{nfo} = \begin{bmatrix} D_x & 0 & 0 \\ 0 & D_y & 0 \\ 0 & 0 & D_z \end{bmatrix} \tag{20}$$

where D_x, D_y and D_z the scalar value of the conductivity tensor in the X , Y and Z direction respectively. The global

conductivity tensor D includes fiber orientation and can be determined using a transformation that involves both D_{nfo} and a rotation matrix R

$$D = RD_{nfo}R^t \tag{21}$$

where R^t is the transpose of rotation matrix R. If each sheet is perpendicular to only one of the global as seen in Fig. 6 (e.g. the x axis in an (x,y,z) coordinate system), then the local basis for each sheet is given by :

$$R_\gamma = \begin{bmatrix} 1 & 0 & 0 \\ 0 & cos\gamma & sin\gamma \\ 0 & sin\gamma & cos\gamma \end{bmatrix} \tag{22}$$

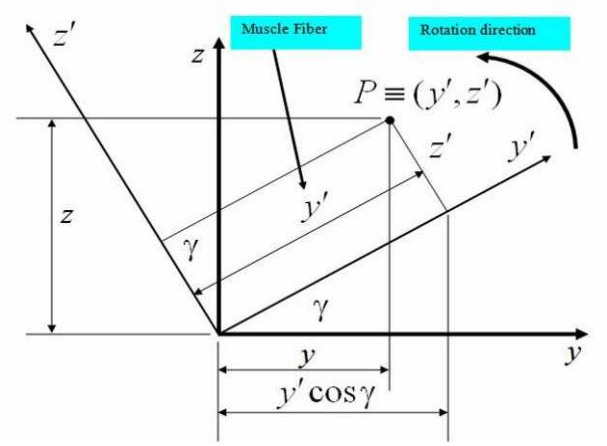

Fig. 6: Schematic representation of idealized fiber rotation about x axis through an angle $\gamma(x)$ to a local basis ($\grave{y}$,$\grave{z}$). Here x-axis represents the heart global longitudinal axis which passes through the apex as shown in Fig.5.

6 Boundrey conditions

In order to specify the boundary conditions, let the closed surface S_H be a boundary separating bidomain region H and surrounding volume conductor B, and let the closed surface S_B bounds region B and n denotes the unit outward normal to S_H and $S_B\phi_\circ$ is the extra cardiac potential, $D_\circ$ is the isotropic scalar conductivity outside of H and n is the outward surface normal of the cardiac [12].

$$\phi_\circ = \phi_e, n.D_\circ\nabla\phi_\circ = n.(D_i\nabla V_m + D_i\nabla\phi_e) On \qquad S_H \tag{23}$$

$$n.D_\circ\nabla\phi_\circ = 0 \qquad On \qquad S_H \tag{24}$$

Since the sources in H are related to the presence of intracellular medium, which is absent in B, we may assume that the vector $D_i\nabla V_m$ in Eq. (23) is tangent to the surface S_H. This becomes the Numan (no flux) boundary conditions [13] which are:

$$n.(D_i\nabla V_m) = 0 \qquad On \qquad S_H \tag{25}$$

$$n.D_e\nabla\phi_e = 0 \qquad On \qquad S_H \tag{26}$$

7 Numerical method and simulation results

The weighted residual method is a technique that can be used to obtain approximate solutions to linear and nonlinear differential equations. If we use this method the finite element equations can be derived directly from the governing differential equations of the problem [14]. The finite element equations is derived using the Galerkin approach.

A Galerkin finite element method is developed to solve the action potential of a cardiac tissue using the monodomain model coupled with the modified FitzHugh-Nagumo (FHN) model on a general domain with equal isotropy and no fiber orientation. Although the implementation supports both two- dimensional (2-D) and three dimensional (3-D) problems, for the simplicity, only 2-D solutions are discussed in this paper.

7.1 Finite element equations

In this sub-section we describe a finite element method (FEM) of the monodomain model which coupled with the modified FitzHugh-Nagumo (FHN) cell model. The monodomain model equation is:

$$\frac{\partial V_m}{\partial t} + \frac{1}{C_m}(I_{ion} - I_{app)} = \left(\frac{1}{C_m\beta_m}\right)\nabla.D\nabla V_m \tag{27}$$

The RHS of the equation (27) is called reaction part and the LHS is called diffusion part. In the case of a single cell model, the diffusion part is non- existent. To solve equation (27), we first expand it as follows:

$$\frac{\partial V_m}{\partial t} + \frac{1}{C_m}(I_{ion} - I_{app)} = \left(\frac{1}{C_m\beta_m}\right)\nabla.\begin{bmatrix} D_x & 0 \\ 0 & D_y \end{bmatrix}\begin{bmatrix} \frac{\partial V_m}{\partial x} \\ \frac{\partial V_m}{\partial y} \end{bmatrix} \tag{28}$$

$$\frac{\partial V_m}{\partial t} + \frac{1}{C_m}(I_{ion} - I_{app)} = \left(\frac{1}{C_m\beta_m}\right)\left[D_x\left(\frac{\partial^2 V_m}{\partial x^2}\right) + D_y\left(\frac{\partial^2 V_m}{\partial y^2}\right)\right] \tag{29}$$

Here, we are applying the Euler method for time derivative and the application of Galerkin method to the diffusion term only over the entire domain Ω of equation (29) as shown in equation (30)

$$\int_\Omega W\frac{\partial V_m}{\partial t}d\Omega = -\int_\Omega W\frac{1}{C_m}(I_{ion} + I_{app})d\Omega$$

$$+\int_\Omega W\left(\frac{1}{C_m\beta_m}\right)\left[D_x\left(\frac{\partial^2 V_m^n}{\partial x^2}\right) + D_y\left(\frac{\partial^2 V_m^n}{\partial y^2}\right)\right]d\Omega \tag{30}$$

where, W is the weighting function. The approximation field variable $\tilde{v}_m$ can be expressed as follows:

$$\tilde{V}_m = \lfloor N_i\rfloor\{V_m\}_i = \lfloor N_1N_2.....N_n\rfloor\{V_m\}_i, W = N \tag{31}$$

where, $\{V_m\}$, the vector of element nodal, i is the grid node index and N is the interpolation function.

Substituting equation (31) into equation (30) gives:

$$\int_\Omega \lfloor N_i \rfloor^T \frac{\partial \tilde{V}_m}{\partial t} d\Omega = -\int_\Omega \lfloor N_i \rfloor^T \frac{1}{C_m} (I_{ion} + I_{app})\, d\Omega + \int_\Omega \lfloor N_i \rfloor^T \left(\frac{1}{C_m \beta_m}\right) \left[D_x \left(\frac{\partial^2 \tilde{V}_m}{\partial x^2}\right) + D_y \left(\frac{\partial^2 \tilde{V}_m}{\partial y^2}\right)\right] d\Omega \quad (32)$$

Using the method of integration by parts, the diffusion term of x-direction in equation (32) is:

$$\int_\Omega \lfloor N_i \rfloor^T \frac{D_x}{C_m \beta_m} \frac{\partial^2 \tilde{V}_m}{\partial x^2} d\Omega = -\int_\Omega \lfloor N_{i,x} \rfloor^T \frac{D_x}{C_m \beta_m} \frac{\partial \tilde{V}_m}{\partial x} d\Omega + \oint_S \lfloor N_i \rfloor^T \frac{D_x}{C_m \beta_m} \frac{\partial \tilde{V}_m}{\partial x} dS \quad (33)$$

Substituting equation (31) into equation (33) gives:

$$\int_\Omega \lfloor N_i \rfloor^T \frac{D_x}{C_m \beta_m} \frac{\partial^2 \tilde{V}_m}{\partial x^2} d\Omega = -\int_\Omega \lfloor N_{i,x} \rfloor^T \lfloor N_i \rfloor \frac{D_x}{C_m \beta_m} \frac{\partial V_m}{\partial x} d\Omega + \oint_S \lfloor N_i \rfloor^T \lfloor N_i \rfloor \frac{D_x}{C_m \beta_m} \frac{\partial V_m}{\partial x} dS \quad (34)$$

where S is the boundary surface of Ω at which the flux is zero. Substituting equation (25) into equation (34) gives:

$$\int_\Omega \lfloor N_i \rfloor^T \frac{D_x}{C_m \beta_m} \frac{\partial^2 \tilde{V}_m}{\partial x^2} d\Omega = -\int_\Omega \lfloor N_{i,x} \rfloor^T \lfloor N_i \rfloor \frac{D_x}{C_m \beta_m} \frac{\partial V_m}{\partial x} d\Omega \quad (35)$$

Again, using the integration by parts method, the diffusion term of y- direction in equation (32) can be expressed by:

$$\int_\Omega \lfloor N_i \rfloor^T \frac{D_x}{C_m \beta_m} \frac{\partial^2 \tilde{V}_m}{\partial y^2} d\Omega = -\int_\Omega \lfloor N_{i,y} \rfloor^T \frac{D_x}{C_m \beta_m} \frac{\partial \tilde{V}_m}{\partial y} d\Omega + \oint_S \lfloor N_i \rfloor^T \frac{D_x}{C_m \beta_m} \frac{\partial \tilde{V}_m}{\partial y} dS \quad (36)$$

Substituting equation (31) into equation (36) gives:

$$\int_\Omega \lfloor N_i \rfloor^T \frac{D_y}{C_m \beta_m} \frac{\partial^2 \tilde{V}_m}{\partial y^2} d\Omega = -\int_\Omega \lfloor N_{i,y} \rfloor^T \lfloor N_i \rfloor \frac{D_x}{C_m \beta_m} \frac{\partial V_m}{\partial y} d\Omega + \oint_S \lfloor N_i \rfloor^T \lfloor N_i \rfloor \frac{D_y}{C_m \beta_m} \frac{\partial V_m}{\partial y} dS \quad (37)$$

where S is the boundary surface of Ω at which the flux is zero. Substituting equation (25) into equation (37) gives:

$$\int_\Omega \lfloor N_i \rfloor^T \frac{D_y}{C_m \beta_m} \frac{\partial^2 \tilde{V}_m}{\partial y^2} d\Omega = -\int_\Omega \lfloor N_{i,y} \rfloor^T \lfloor N_i \rfloor \frac{D_y}{C_m \beta_m} \frac{\partial V_m}{\partial y} d\Omega \quad (38)$$

After substitution equations (35) and (38) into equation (32) and applying the Euler method for time derivative, the resulting algebraic equation represented by matrix form is obtained as follows:

$$(V_m)_i^{n+1} = (V_m)_i^n - \left([M]^{-1}[K](V_m)_i^n + S_i^n\right) \Delta t \quad (39)$$

where the superscript n is time index, M is the FEM lumped mass matrix and K is the FEM stiffens matrix.

7.2 Spliting of operators and the solution procedure

When solving a system of ODEs or PDEs, it may be inefficient to use one numerical method for every part of the system [3]. For example, some components of the system may be most efficiently solved with one numerical method and other parts of the system most efficiently solved with another numerical method. Rather than solving such a system with one numerical method and accepting the consequences of inefficiency, it is often better to use a splitting method [10]. A splitting method uses a divide-and-conquer strategy to solve the system by breaking the system into parts that can be solved efficiently with one particular method. For instance, in splitting process and solution sequence of the current simulation can be summarized as follows.

Step 1: for a time step $\Delta t/2$ we solving the diffusion equation

$$\frac{\partial V_m}{\partial t} = \left(\frac{1}{C_m \beta_m}\right) \left[D_x \left(\frac{\partial^2 V_m}{\partial x^2}\right) + D_y \left(\frac{\partial^2 V_m}{\partial y^2}\right)\right] \quad (40)$$

$$(V_m)_i^{n+1} = (V_m)_i^{n+1/2} - \left([M]^{-1}[K](V_m)_i^{n+1/2}\right) \Delta t \quad (41)$$

Step 2: for a time step Δt we solving the reaction equation

$$\frac{\partial V_m}{\partial t} = -\frac{1}{C_m}(I_{ion} + I_{app}) \quad (42)$$

$$(V_m)_i^{n+3/2} = (V_m)_i^{n+1} + S_i^{n+1} \Delta t \quad (43)$$

Step 3: for a time step ($3\Delta t/2$) we solving the diffusion equation

$$\frac{\partial V_m}{\partial t} = \left(\frac{1}{C_m \beta_m}\right) \left[D_x \left(\frac{\partial^2 V_m}{\partial x^2}\right) + D_y \left(\frac{\partial^2 V_m}{\partial y^2}\right)\right] \quad (44)$$

Here V_m in RHS is the result of step 2.

$$(V_m)_i^{n+2} = (V_m)_i^{n+3/2} - \left([M]^{-1}[K](V_m)_i^{n+3/2}\right) \Delta t \quad (45)$$

Step 4: repeat steps 1- 3 until the desired solution is obtained.

7.3 Simulation results

7.3.1 Discretization of the tissue

In this section we present the results which obtained by the MATLAB code to generate the uniform mesh for the heart tissue as a triangular element and a rectangle element. The first step in the finite element method is to divide the structure or solution region into subdivisions or

elements. Hence, the structure is to be modeled with suitable finite elements. The number, type, size, and arrangement of the elements are to be decided.

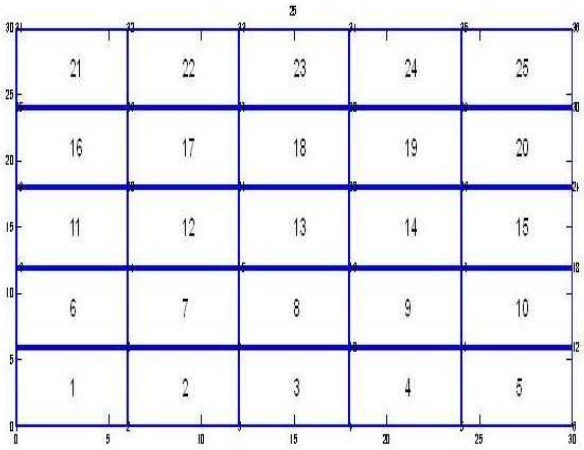

Fig. 7: The uniform mesh for the heart tissue as a rectangle element.

We consider two dimensional domains (heart tissues). Figure 7 represents the uniform mesh for the heart tissue as a rectangle element and Fig. 8 represents the uniform mesh for the heart tissue as a triangle element. In case for the same dimensional of the tissue, we find the number of element in triangle is double rectangle element.

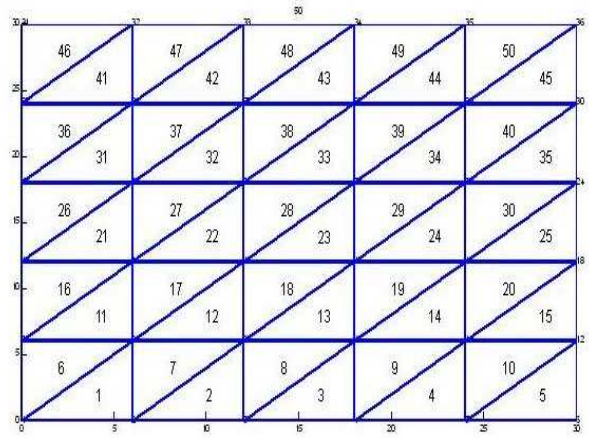

Fig. 8: The uniform mesh for the heart tissue as a triangle element.

7.3.2 Numerical simulations

In this sub-section we present the results of the numerical simulations. Here, we consider two dimensional domains ($10 * 10mm$ heart tissues). We run coupled cell model monodomain simulations, with the modified FHN. In the numerical simulations we have been used the parameter which shown in Table 1 for the modified FitzHugh-Nagumo model. Figure 9 represents the reference action potential and the simulation of action potential for a monodomain cell with rectangle element. Figure 10 represents the reference action potential and the simulation of action potential for a monodomain cell with triangle element. In Fig. 9 and 10, the tissue has a negative resting potential, typically $v = -90mV$. The signal propagation in the heart takes the form of a depolarization, where the potential rises rapidly and reaches a positive peak potential after a couple of milliseconds. A plateau phase follows, where the potential remains positive for a little more than 100 ms. Finally, the cell depolarizes, returning to its negative resting potential. The whole process is called the action potential and typically lasts around 300 ms. We compute the error between the reference action potential and our simulation of action potential for a monodomain cell with rectangle element and triangle element.

Results show that the uniform mesh for the heart tissue as a triangular element is better in the result than we used the uniform mesh for the heart tissue as a rectangular element. This may be referred to that; the number of element in triangle is double rectangle element for the same dimensional of the cardiac tissue. The simulation errors are depicted in Fig 11. We also computed the relative root-mean square error (E_{RMS}) between the numerical solutions V_m and the reference V_m^{ref} which can be computed by using the equation 46 to give a more intuitive sense of the error between the reference action potential and our simulation of action potential for a monodomain cell with rectangle element and triangle element. We find the E_{RMS} when we use the uniform mesh for the heart tissue as a triangular element is less than the result we used the uniform mesh for the heart tissue as a rectangular element, Table 2. In the two cases, the relative root-mean square error is less than 5%, which is generally considered acceptable.

$$E_{RMS} = \sqrt{\frac{\sum_{i=1}^{n}\left(V_i - V_{ii}^{ref}\right)^2}{\sum_i^n V_i^{ref^2}}} \qquad (46)$$

Table 1: Values of the parameters in the modified FitzHugh-Nagumo model [3, 15].

Parameter	Description	Value	Unites
β_m	the surface area- to-volume ratio	200	mm^{-1}
C_m	cell capacitance per unite surface area	0.01	$\mu F\ mm^{-2}$
C	Excitation rate constant	0.002	$mA\ mm^{-2}$
E	Recovery rate constant	0.002	ms^{-1}
ε	Recovery decay constant	0.5	Dimensionless
V_{rest}	Resting potential	-85	mV
V_{th}	Threshold potential	-75	mV
V_p	Plateau potential	15	mV

Table 2: E_{RMS} values for two types of element rectangle element and triangle element.

Element type	E_{RMS}
Rectangle Element	0.02005
Triangle Element	0.01559

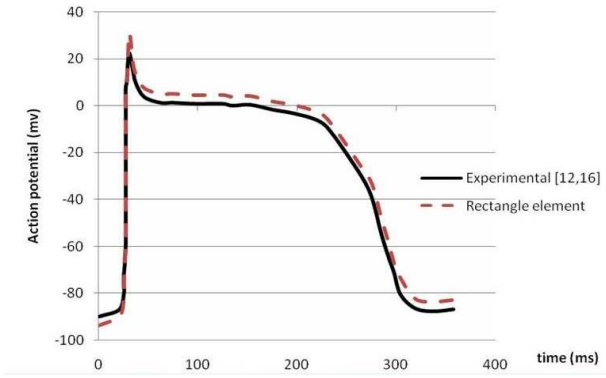

Fig. 9: The solid line represents the reference action potential and the dotted line represents the simulation of action potential for a monodomain cell with rectangle element.

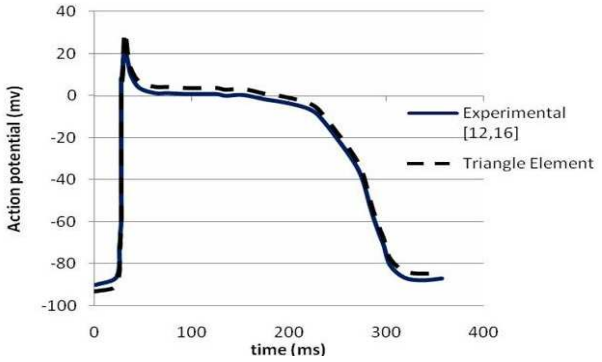

Fig. 10: The solid line represents the reference action potential and the dotted line represents the simulation of action potential for a monodomain cell with triangle element.

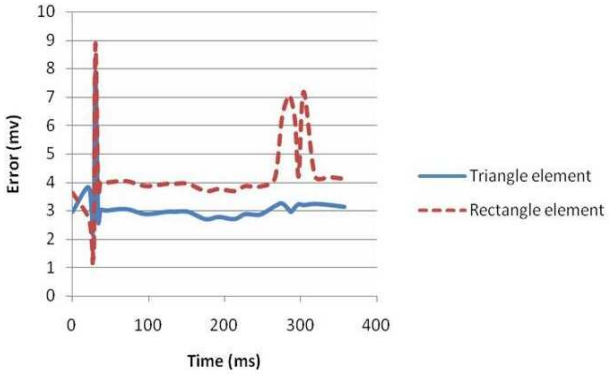

Fig. 11: The error versus time

8 Conclusions

In this paper, an approach is presented to simulate the propagation of the excitation in the cardiac tissues, based on non linear models of reaction-diffusion type, considering the monodomain approach. The ionic currents are expressed by the simple modified electrophysiological cell model (FHN model), especially designed for human tissues. Numerical simulations on a two dimensional domain ($10 * 10mm$ heart tissues) were simulated to show the behavior of the excitation spread and the repolarization phase for isotropic electric activity. The results show that the proposed developed code can successfully be used to simulate heart excitation isotropic propagation in two-dimensional tissue and it suggests that such method may provide a good basis for heart simulation research in a more physiologically way. The present developed code helps calculate the intra-cellular and extra-cellular action potential of human cardiac tissues in the heart physical domain which can be used to predict the cardio electrocardiograph (ECG).

References

[1] Ricardo Silva Campos, Marcelo Lobosco, Rodrigo Weber dos Santos" Adaptive Time Step for Cardiac Myocyte Models " International Conference on Computational Science, ICCS (2011)

[2] D.Noble."Modelling the heart insights, failures and progress", Bioessays **24**, 1155-63 (2002) .

[3] J.Sundnes, G.T.Lines, X.Cai, B.F.Nielsen, K.-A.Mardal, and A.Tveito. "Computing the Electrical Activity in the Heart". Springer-Verlag, Berlin, (2006).

[4] C.S.Henriquez. "Simulating the electrical behavior of cardiac tissue using the Bidomain model". Crit. Rev. Biomedical. Engineering **21**, 1-77 (1993).

[5] J.M.Rogers and A.D.McCulloch.”A collocation - Galerkin nite element model of cardiac action potential propagation”. IEEE Trans. Biomedical. Engineering **41**, 743-57 (1994) .
[6] Yu Zhang, Ling Xia, Yinglan Gong, Ligang Chen, Guanghuan Hou and Min Tang.”Parallel Solution in Simulation of Cardiac Excitation Anisotropic Propagation,” FIMH, LNCS **4466**, 170-179 (2007).
[7] Olivier BLANC”A computer Model Of Human Atrial Arrhythmia” **2537**, (2002)
[8] Qingyun Wang, Qishao Lu, GuanRong Chen, Zhaosheng feng and LiXia Duan ”Bifurcation and synchronization of synaptically coupled FHN models with time delay” Chaos, Solitons and Fractals **39**, 918-925 (2009)
[9] A.J.Pullan, M.L.Buist, and, and L.K.Cheng.”Mathematically Modelling the Electrical Activity of the Heart: From Cell to Body Surface and Back Again. World Scientic, New Jersey (2005) .
[10] E.J.Vigmond, R.W.dosSantos, A.J.Prassl, M.Deo, and G.Plank.”Solvers for the cardiac Bidomain equations”. Progress in Biophysics Molecular Biology **96**, 318 (2008)
[11] Barr, R. C. and Joseph D. Bronzino ”Basic Electrophysiology.”The Biomedical Engineering Handbook: Second Edition. Boca Raton: CRC Press LLC, (2000).
[12] Yu Zhang, Ling Xia and Guanghuan Hou”Efficient Solution of Bidomain Equations in Simulation of Cardiac Excitation Anisotropic Propagation,” ICIC, LNBI **4115**, 571-581 (2006).
[13] R.H.Clayton, O.Bernus, E.M.Cherry, H.Dierckx, F.H.Fenton, L.Mirabella, ”Models of cardiac tissue electrophysiology Progress, Challenges and open questions. Progress in Biophysics Molecular Biology **48**, 104-22 (2011) .
[14] Singiresu S.RAO.”The Finite Element Method In Engineering”Fourth Edition, ISBN: 0750678283, Elsevier Science & Technology Books, December (2004).
[15] Maria Murillo And Xiao-Chuan Cai ”A fully implicit parallel algorithm for simulating the non-linear electrical activity of the heart”Numer. Linear Algebra Appl **11**, 261-277 (2004) .
[16] Frank B. Sachse ”Computational Cardiology” ISSN 0302-9743 Springer-Verlag, Berlin Heidelberg, (2004).